Cooperative Adaptive Fault-Tolerant Formation Control of Quadrotor Swarm with Cyber-Attacks

Sh. Hadizadeh[1], V. Nekoukar[2*], and N. Mahdian Dehkordi[3]

[1] Departments of Control, School of Electrical Engineering, Shahid Rajaee Teacher Training University, Iran (e-mail: sh.hadizade@gmail.com).

[2] Departments of Control, School of Electrical Engineering, Shahid Rajaee Teacher Training University, Iran (e-mail: v.nekoukar@sru.ac.ir).

[3] Departments of Control, School of Electrical Engineering, Shahid Rajaee Teacher Training University, Iran (e-mail: nimamahdian@sru.ac.ir).

*Corresponding Author

Abstract— **The unique features of multi-rotor unmanned aerial vehicles (MRUAVs) have led to a variety of applications. However, the carrying capacity of MRUAVs remains one of the most critical challenges. Forming an MRUAV swarm can be an effective solution. In MRUAV swarms, followers require a formation control scheme to track one or more leaders. This formation control must address measurement noise, communication delays, model uncertainty, actuator and sensor faults, and cyber-attacks. In this paper, we propose a new cooperative adaptive fault-tolerant formation control for quadrotor swarms in the presence of deception during cyber-attacks. Quadrotors are connected to neighboring drones and a central leader. We evaluate the proposed method's ability to handle model uncertainty, actuator faults, cyber-attacks, and measurement noise through simulation studies. Considering all these challenges simultaneously and evaluating the presented formation control method stand as one of the primary contributions of this paper.**

Keywords: **Cooperative control, fault-tolerant, formation control, quadrotor, unmanned aerial vehicle.**

I. INTRODUCTION

IN recent years, the industrial and research applications of multi-rotor unmanned aerial vehicles (MRUAVs) have witnessed significant development. This popularity is largely attributed to the small size, simple structure, low price, and flight capability of MRUAVs, which find use in surveillance, air traffic control, firefighting, exploration, and various missions related to telecommunications, geography, and espionage [1].

However, certain applications, such as firefighting or search and rescue, cannot be effectively carried out by a single MRUAV. These missions necessitate the formation of an MRUAV swarm. When multiple MRUAVs collaborate, they can execute complex tasks with remarkable efficiency and heightened reliability, surpassing what a high-tech, expensive fixed-wing drone can achieve. Compared to individual MRUAVs, an MRUAV swarm offers several advantages, including scalability, survivability, and redundancy [2, 3].

The drone swarm can consist of several MRUAVs that communicate and collaborate with each other as a multi-agent system. Both the leader and followers must maintain a stable swarm formation. Therefore, the performance of formation control is crucial. The followers should adhere to the formation, track their leader, and avoid collisions. Formation control methods need to address communication and measurement noise, communication delays, model uncertainty, topology changes, actuator and sensor faults, and deception in cyber-attacks.

Recently, researchers have investigated various cooperative formation control methods of drone swarms in the presence of sensor noises, actuator faults, and attacks to guarantee the reliability and robustness of closed-loop systems [4]. There are many types of actuator faults including bias, loss of effectiveness, and outage [5]. The cyber-attack can also affect the system operation by changing the system data or injecting false data [4, 6]. Since the formation control needs coordination between MUAVs, the sensor noises also decrease the efficiency of the formation control [7].

The problem considered here is to provide a formation control method for MRUAVs that can deal with actuator faults and deception attacks. In recent research, optimal

control [8, 9], output feedback [10], fuzzy control [11-14], sliding mode control [15-18], adaptive control [5, 19-29], and impulsive control methods [30] have been applied to deal with the aforementioned challenges.

In [31], a time-varying formation control of UAV swarms was presented based on switching-directed topologies. The authors considered only the relative information of neighbor UAVs. Deng and his colleagues proposed a method that applies comparative states of the fixed-wing UAV and its neighboring to design fault observers, instead of using states of each UAV, directly [32]. In [3], the authors designed a multi-UAV system of quadrotors and applied a decentralized model predictive formation control. An acceptable performance was achieved by estimation of system delays and disturbances using a nonlinear model of UAV. Yuan and his colleagues studied the UAV formation consolidation and fault tolerance where the formation changes consecutively amongst several forms [33]. The number and combination of UAVs may switch between these forms, and some UAVs may have faults. Wang et al investigated the leader-following swarm problem of UAV systems with uncertainty, actuator fault, and nonlinear dynamics and suggested a group of distributed consensus protocols based only on the relative states among neighbor UAVs [34].

In [35], a consensus theory was applied to address the robust leaderless time-varying formation and trajectory tracking issues of UAV swarm systems with the Lipschitz nonlinear dynamics and external disturbances under directed switching topologies. A decentralized navigation strategy for UAVs was proposed by using neighboring information via the communication network in [36]. A task reassignment and formation reconstruction algorithm were also developed based on the distributed Hungarian algorithm to deal with practical limitations such as the unknown disturbances, loss of team members, and obstacle avoidance.

In most previous studies, faults and attacks were not considered simultaneously. Additionally, in simulations, the nonlinear dynamic model of quadrotors was considered as a linear model, and the effects of measurement noise were not studied.

In this paper, a cooperative adaptive fault-tolerant controller is proposed to control the formation of a quadcopter swarm. In the controller design, actuator faults and deception in cyber-attacks are considered simultaneously. Followers are connected to the leader and their neighbors. They take the coordination information and adjust their position, accordingly. The distance between the leader and followers and the followers with each other is a predetermined value. For designing the proposed cooperative control, every agent

is assumed as a double integrator but, in the simulation, the dynamic model of quadcopters is considered as the model introduced in [37]. An impulsive method is presented to eliminate cyber-attack. Also, an adaptive fault-tolerant control method is proposed to deal with the actuator fault. In the simulation studies, the performance of the proposed control scheme is evaluated in the presence of actuator fault, cyber-attack, model uncertainty, and measurement noise.

II. DYNAMIC MODEL OF QUADROTOR

In this section, the dynamics of the quadrotor is introduced, and the six-degree freedom model of the drone is presented. The resultant forces of the spinning rotors on the drone determine quadrotor position in space. If $[x \quad y \quad z]^T$ is the position vector of the quadrotor and $[\phi \quad \theta \quad \psi]^T$ is the vector of $X - Y - Z$ Euler angles, the six-degree freedom dynamic equations of the quadrotor can be written as (1) to (6) [37].

$$\ddot{x} = F_{A,x} + (\cos \psi \sin \theta \cos \phi + \sin \psi \sin \phi) \frac{T}{m} \quad (1)$$

$$\ddot{y} = F_{A,y} + (\sin \psi \sin \theta \cos \phi + \sin \phi \sin \psi) \frac{T}{m} \quad (2)$$

$$\ddot{z} = F_{A,z} - g + (\cos \theta \cos \phi) \frac{T}{m} \quad (3)$$

$$\dot{p} = \tau_{A,x} + \frac{I_r}{I_x} q\Omega_r + \frac{I_y - I_z}{I_x} qr + \frac{\tau_\phi}{I_x} \quad (4)$$

$$\dot{q} = \tau_{A,y} + \frac{I_r}{I_y} p\Omega_r + \frac{I_z - I_x}{I_y} pr + \frac{\tau_\theta}{I_y} \quad (5)$$

$$\dot{r} = \tau_{A,z} + \frac{I_x - I_y}{I_z} pq + \frac{\tau_\psi}{I_z} \quad (6)$$

where p, q, and r are the angular velocity in the body fixed frame, which are measured by gyroscope sensors. $F_{A,x}$, $F_{A,y}$, and $F_{A,z}$ and $\tau_{A,x}$, $\tau_{A,y}$, and $\tau_{A,z}$ are external force and torque disturbances, respectively. m and g are the total mass of the quadrotor and the gravitational constant, respectively. I_x, I_y, and I_z are the moment of inertia around $X - Y - Z$. I_r is the inertial moment of rotors. The total thrust T and total torques τ_ϕ, τ_θ, and τ_ψ are calculated by

$$\begin{bmatrix} T \\ \tau_\phi \\ \tau_\theta \\ \tau_\psi \end{bmatrix} = \begin{bmatrix} 1 & 1 & 1 & 1 \\ 0 & h & 0 & -h \\ h & 0 & -h & 0 \\ -c_\tau & c_\tau & -c_\tau & -c_\tau \end{bmatrix} \begin{bmatrix} f_1 \\ f_2 \\ f_3 \\ f_4 \end{bmatrix} \quad (7)$$

$$f_i = b_i \Omega_i^2 \qquad i = 1, 2, 3, 4 \quad (8)$$

that h is the distance from the center of mass to the center of each rotor. c_τ is a fixed constant and f_i is the thrust generated by ith rotor along z axis. Ω_r is determined by

$$\Omega_r = \Omega_1 - \Omega_2 + \Omega_3 - \Omega_4 \qquad (9)$$

where Ω_i is the rotational speed of ith rotor which has a proportional relation with the rotor voltage. The Euler angles are obtained by solving the following differential equations.

$$\dot{\phi} = p + q \sin\phi \tan\theta + r \cos\phi \tan\theta \qquad (10)$$

$$\dot{\theta} = q \cos\phi - r \sin\phi \qquad (11)$$

$$\dot{\psi} = q \sin\phi \sec\theta + r \cos\phi \sec\theta \qquad (12)$$

III. FAULT-TOLERANT COOPERATIVE CONTROL

The objective of the cooperative control is to obtain a predefined formation of MRUAVs in the presence of deception and actuator bias faults. Under cyber-attacks, false data will be entered into the communication channels. So, accurate synchronization is impractical to be attained. In this section, an impulsive controller is presented to eliminate deception. Also, to compensate for the actuator faults, an adaptive fault-tolerant control is proposed.

To implement the control scheme, the nonlinear model presented in the previous section is simplified as equations (13) to (18) [38]. Then, it is transformed into a linear double-integrator model by feedback linearization [39].

$$\ddot{x} = -\sin\theta \cos\phi \frac{T}{m} \qquad (13)$$

$$\ddot{y} = \sin\phi \frac{T}{m} \qquad (14)$$

$$\ddot{z} = g - \cos\theta \cos\phi \frac{T}{m} \qquad (15)$$

$$\ddot{\phi} = \frac{\tau_\phi}{I_x} \qquad (16)$$

$$\ddot{\theta} = \frac{\tau_\theta}{I_y} \qquad (17)$$

$$\ddot{\psi} = \frac{\tau_\psi}{I_z} \qquad (18)$$

Matrices A and B are defined as follows.

$$A = \begin{bmatrix} 0 & 1 & 0 & 0 \\ 0 & 0 & 0 & 0 \\ 0 & 0 & 0 & 1 \\ 0 & 0 & 0 & 0 \end{bmatrix} \qquad B = \begin{bmatrix} 0 & 0 \\ 1 & 0 \\ 0 & 0 \\ 0 & 1 \end{bmatrix} \qquad (19)$$

So, the dynamics of the leader is described by

$$\dot{p}_0(t) = A p_0(t) + B u_0(t) \qquad (20)$$

$$p_0(t) = [x_0(t) \quad \dot{x}_0(t) \quad y_0(t) \quad \dot{y}_0(t)]^T \qquad (21)$$

where $p_0(t)$ and $u_0(t)$ denote the state of the leader and the control input, respectively. The dynamics of ith follower is explained by

$$\dot{p}_i(t) = A p_i(t) + B u_i(t) \qquad (22)$$

$$p_i(t) = [x_i(t) \quad \dot{x}_i(t) \quad y_i(t) \quad \dot{y}_i(t)]^T \qquad (23)$$

Here, $p_i(t)$ defines the state of ith follower. The control input $u_i(t)$ is defined as

$$u_i(t) = u_{i1}(t) + u_{i2}(t) \qquad (24)$$

$$u_{i1}(t) = K_1 e_i \qquad (25)$$

$$\varepsilon_i(t) = p_i(t) - p_o(t) \qquad (26)$$

$$e_i = \sum_{j \in N_i} a_{ij} \left(p_j(t) - p_i(t) \right) - g_i \varepsilon_i(t) \qquad (27)$$

$$u_{i2}(t) = -K_2 \left[\sum_{j \in N_i} a_{ij} \left(p_j(t) - p_i(t) \right) - g_i \varepsilon_i(t) \right] \qquad (28)$$

where K_1 and K_2 are the feedback gain matrices. $\varepsilon_i(t)$ and e_i are defined as the tracking error and local neighborhood consensus error, respectively. a_{ij} and g_i are elements of the follower adjacency matrix F and leader adjacency matrix L, respectively.

A. Model of Actuator Fault and Cyber-Attack

If an actuator bias fault occurs, and a cyber-attack injects into the communication network between agent i and its neighbor agents, then the model of the fault and cyber-attack can be written as

$$u_{i1}^F = u_{i1} + \varphi_i \qquad (29)$$

$$u_{i2}^F(t) = -K_2 \left[\sum_{j \in N_i} \left(a_{ij} \left(p_j(t) - p_i(t) \right) + \gamma_{ij} q_i \right) - g_i \varepsilon_i(t) \right] \tag{30}$$

where φ_i is a constant and shows bounded bias fault of actuators and $\bar{\Phi} = diag[\varphi_1, \varphi_2, \dots \varphi_N]$. γ_{ij} indicates the decision variable of an attacker. $\gamma_{ij} = 1$ represents that the attacker launches the attack, otherwise $\gamma_{ij} = 0$. $q_i(t)$ is the attack signal sent by attackers which are energy-limited, $Q(t) = [q_1^T, q_2^T, \dots, q_N^T]^T$ satisfying $\|Q(t)\|^2 \le q$, that q is a known positive constant.

It is supposed that the deception in the cyber-attack is defined by one independent random variable γ_{ij} that obeys the Bernoulli distribution as

$$\text{Prob } \{\gamma_{ij}(t) = 1\} = \lambda_{ij} \tag{31}$$

$$\text{Prob } \{\gamma_{ij}(t) = 0\} = 1 - \lambda_{ij} \tag{32}$$

Here, $\lambda_{ij} \epsilon [0,1)$ is a constant and $\gamma_{ii} = 0$.

B. Model of Actuator Fault and Cyber-Attack

Exact synchronization is impossible to be achieved under deception and actuator faults. So, we need a cooperative fault-tolerant controller for eliminating their effects. For this purpose, an adaptive fault-tolerant control is presented as

$$u_{i1}^c(t) = d_i(t) \left[\sum_{j \in N_i} a_{ij} \left(p_j(t) - p_i(t) \right) - g_i \varepsilon_i(t) \right] \tag{33}$$

The update law of adaptive parameters is described by

$$\dot{d}_i(t) = -v(\|PB\| \|e_i(t)|^2 + d_i(t)) \tag{34}$$

where $v > 0$ is a constant and P is a positive definite matrix. $\bar{d} = diag[d_1, d_2, \dots d_N]$ and $\|d_i(t)\| \le d_m$. Also, there is a positive constant l that satisfies

$$l > \|PA(L + F)^{-1}\| \tag{35}$$

$$(d_i + l)d_i > \|B\bar{\Phi}\| \tag{36}$$

An impulsive controller is applied to compensate cyber-attacks defined by

$$u_{i2}^c(t) = -\sum_{k=1}^{\infty} K_2 \left[\sum_{j \in N_i} \left(a_{ij} \left(p_j(t) - p_i(t) \right) + \gamma_{ij} q_i \right) - g_i \varepsilon_i(t) \right] \delta(t - t_k) \tag{37}$$

that $\delta(.)$ is Dirac impulse and the impulse sequence $\{t_k\}_{k=1}^{\infty}$ satisfies $0 = t_0 < t_1 < \dots < \infty$.

Theorem 1. The following control law

$$u_i(t) = u_{i1}^c(t) + u_{i2}^c(t) \tag{38}$$

guarantees that the quadcopter swarm with a leader and arbitrary followers achieves consensus in the presence of cyber-attacks and actuator faults.

Proof. Consider the Lyapunov function $V(t)$ as

$$V(\varepsilon(t)) = \frac{1}{2} \varepsilon(t)^T (L + F) \otimes P \varepsilon(t) \tag{39}$$

that $\otimes$ denotes the Kronecker product. The infinitesimal operator $\mathcal{L}$ of $V(\varepsilon(t))$ [40, 41] can be written as (40) when $t \ne t_k$, for $t \in [t_k, t_{k-1})$, $k = 1,2, \dots$.

$$\begin{aligned}
\mathcal{L}V(\varepsilon(t)) &= \varepsilon(t)^T (L + F) \otimes P \big[(I_N \otimes A)\varepsilon(t) \\
&\quad + (I_N \otimes B) \big((L + F) \otimes \bar{d} \big) \varepsilon(t) + (I_N \otimes B)\bar{\Phi} \big] \\
&= \varepsilon(t)^T (L + F) \otimes PA\varepsilon(t) \\
&\quad + \varepsilon(t)^T (L + F) \otimes PB(L + F) \otimes \bar{d}\varepsilon(t) + (I_N \otimes B)\bar{\Phi}
\end{aligned} \tag{40}$$

By considering (35) and (36), we have

$$\begin{aligned}
\dot{V}(t) &\le \varepsilon(t)^T (L + F) \otimes PA\varepsilon(t)(L + F)(L + F)^{-1} \\
&\quad + \varepsilon(t)^T (L + F) \otimes PB(L + F) \otimes \bar{d}\varepsilon(t) + (I_N \otimes B)\bar{\Phi} \\
&\quad - \sum_{i=1}^{N} (d_i + l)(\|PB\| \|e_i(t)\|^2 + d_i) \\
&\le \sum_{i=1}^{N} (e_i(t))^T PA (L + F)^{-1} e_i(t) \\
&\quad + (e_i(t))^T PB d_i e_i(t) + B\varphi_i \\
&\quad - (d_i + l)(\|e_i(t)\|^2 + d_i)
\end{aligned} \tag{41}$$

We have $l > \|PA(L + F)^{-1}\| + \|PB(L + F)^{-1}\|$ and $(d_i + l)d_i > \|B\bar{\varphi}_i\|$ where $\|\bar{\varphi}_i\| \ge \|\varphi_i\|$. Therefore $\dot{V}(t) < 0$ and $E\{\dot{V}(t)\} < 0$, and consequently

$$E\{V(t)\} < \rho E\{V(t_{k-1})\}, t \in [t_{k-1}, t_k) \qquad (42)$$

where $0 < \rho < 1$. $E\{V(t)\}$ is the expectation of $V(t)$. Define $M = I_N - (I_N \otimes B)(L+F) \otimes I_N \otimes K$ and $W = (I_N \otimes K)(\Upsilon \otimes I_N)Q$ that $\Upsilon = [\gamma_{ij}]_{N \times N}$. For $t = t_k$, we have

$$\varepsilon(t_k) = M\varepsilon(t_k^-) + W(t_k) \qquad (43)$$

So,

$$
\begin{aligned}
& E\{V(\varepsilon(t_k^+))\} = E\{V(\varepsilon(t_k))\} \\
&= E\{\varepsilon^T(t_k^+)M^T + W(t_k)[(L+F) \otimes P]M\varepsilon(t_k^-) \\
&\quad + W(t_k)\} \\
&= E\{\varepsilon^T(t_k^-)M^T[(L+F) \otimes P]M\varepsilon(t_k^-) \\
&\quad + \varepsilon^T(t_k^-)M^T[(L+F) \otimes P]W(t_k) \\
&\quad + W^T(t_k)[(L \\
&\quad + F) \otimes P]M\varepsilon(t_k^-) + W^T(t_k)[(L \\
&\quad + F) \otimes P]W(t_k)\}
\end{aligned} \qquad (44)
$$

$$
\begin{aligned}
E\{\varepsilon^T(t_k^-)M^T[(L+F) \otimes P]M\varepsilon(t_k^-)\} \\
= E\{\varepsilon^T(t_k^-)[I_N \\
- (I_N \otimes B)(L \\
+ F) \otimes I_N \otimes K]^T . [I_N \\
- (I_N \otimes B)(L \\
+ F) \otimes I_N \otimes K][(L \\
+ F) \otimes P]\varepsilon^T(t_k^-)\} \\
\leq \bar{S}_1^{\ 2} E\{V(\varepsilon(t_k^-))\}
\end{aligned} \qquad (45)
$$

$$
\begin{aligned}
& E\{\varepsilon^T(t_k^-)M^T[(L+F) \otimes P]W(t_k) \\
& + W^T(t_k)[(L+F) \otimes P]M\varepsilon(t_k^-)\} \\
& \leq E\left\{\varepsilon^T(t_k^-)[(L+F) \otimes P]\varepsilon(t_k^-)\right\} \\
& + E\left\{Q(t_k)(\Upsilon^T(t_k)(I_N \otimes BK)^T[I_N \right. \\
& - (I_N \otimes B)(L \\
& + F) \otimes K].[I_N \\
& \left. - (I_N \otimes B)(L+F) \otimes K]^T(I_N \otimes BK)\Upsilon(t_k)\right\} \\
& \leq E\{V(\varepsilon(t_k^-)) + q\lambda_{max}\}.\bar{S}_2^{\ 2}
\end{aligned} \qquad (46)
$$

$$
\begin{aligned}
& E\{W^T(t_k)((L+F) \otimes P)W\} \\
& \leq E\{Q^T(t_k)\Upsilon^T(t_k) \otimes BK^T((L \\
& + F) \otimes P)(BK)^T \otimes \Upsilon^T(t_k)Q(t_k)\} \leq q\lambda_{max}\bar{S}_2^{\ 2}
\end{aligned} \qquad (47)
$$

where λ_{max} is the maximum eigenvalue of $[(L+F) \otimes P]$. $\bar{S}_1$ and $\bar{S}_2$ are maximum singular values of $[I_N - (I_N \otimes B)(L+F) \otimes K]$ and $[\Psi^T(I_N \otimes BK)^T]$, respectively. Ψ is defined as

$$\Psi = E[\Upsilon(t_k)] \qquad (48)$$

By combining (44) to (47), it can be written as

$$
\begin{aligned}
E\{V(\varepsilon(t_k^+))\} \leq \bar{S}_1^{\ 2} E\{V(\varepsilon(t_k^-))\} \\
+ q^2\lambda_{max}\bar{S}_2^{\ 2} + q^2\lambda_{max}\bar{S}_3^{\ 2}
\end{aligned} \qquad (49)
$$

that $\bar{S}_3$ is the maximum singular value of $[\Psi^T(I_N \otimes BK)^T(I_N - (I_N \otimes B))(L+F) \otimes K]$. So, we have

$$
\begin{aligned}
E\{V(\varepsilon(t_k))\} \leq \bar{S}_1^{\ 2} E\{V(\varepsilon(t_k^-))\} \\
+ q^2\lambda_{max}\bar{S}_2^{\ 2} + q^2\lambda_{max}\bar{S}_3^{\ 2}
\end{aligned} \qquad (50)
$$

According to (42) and (50)

$$
\begin{aligned}
E\{\|\varepsilon(t)\|^2\} &\leq \frac{1}{\|(L+F) \otimes P\|} E\{V(\varepsilon(t))\} \\
&\leq \frac{1}{\|(L+F) \otimes P\|} \frac{\rho\left(1 - \bar{S}_1^{\ 2}\right)\sum_{i=1}^N \frac{1}{\nu}\left(\bar{d}_m + l\right)^2}{2\left(1 - \bar{S}_1^{\ 2}\right)} \\
&+ \Delta q^2\lambda_{max}\bar{S}_2^{\ 2} + q^2\lambda_{max}\bar{S}_3^{\ 2}
\end{aligned} \qquad (51)
$$

Therefore, the amplitude of the tracking error is bounded, and consensus of quadcopter swarm is achieved. ∎

IV. SIMULATION

Simulation results are given to evaluate the effectiveness of the proposed method. A quadrotor swarm with a leader and eight followers is considered. The desired distance between the leader and followers and followers with each other are predetermined values along the X and Y axis even in their initial condition. The trajectory of the leader is predefined. The value of Z and ψ state variables is equal to the leader for all followers. The closed-loop control structure of the leader and followers is presented in Fig. 1. Six PID controllers are applied for control of the position and attitude of the leader. Three PID controllers control the position, and the other ones control the attitude of the leader quadcopter. For the followers, the control framework consists of four PID controllers and the proposed cooperative adaptive fault-tolerant formation controller. Three PID controllers control the follower attitude, a PID controls the height of the followers, and the proposed formation controller maintains the formation by calculating the references of the pitch (θ_{ref}) and roll (ϕ_{ref}) of the followers.
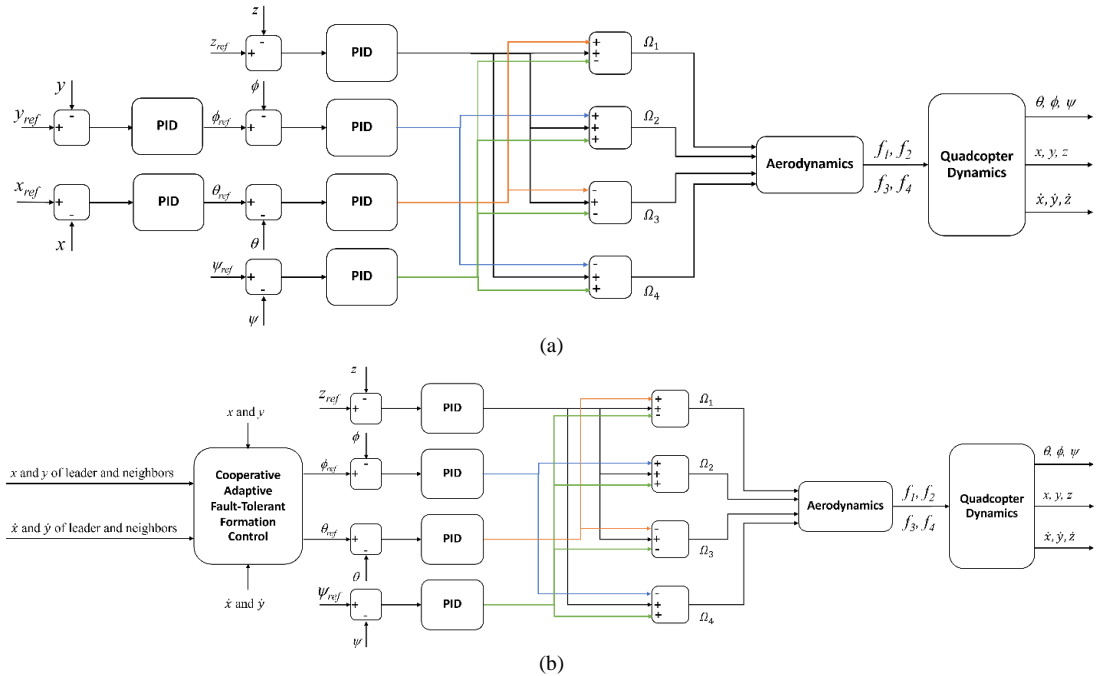
(a)

(b)

Fig. 1. Closed-loop control structure of the quadcopter for (a) leader and (b) followers.

Agent 1 represents the leader and agents 2-9 represent the followers. Agents 2-5 communicate with the leader and their neighbors and agent 6-9 are only in contact with their neighbors. The communication graph topology is shown in Fig. 2. The shown arrows indicate the direction of sending data. For example, the leader sends its position to followers 2, 3, 4 and 5. The maximum values of the fault and attack are selected 2 degrees and 0.2 meters, respectively. The primary issue with the quadcopter faults is related to its motors and challenges in controlling the quadcopter's attitude. If this fault doesn't cause the quadcopter's instability, it triggers a shift in its attitude, rendering control more challenging. Consequently, in this study, presuming the proper functioning of motors and attitude controllers, the impact of the fault is directly evaluated with respect to the intended desirable attitude. The simulation is performed based on parameters of the quadrotor that are given in Table I in two different scenarios. The matrices F and L are defined as

$$F = \begin{bmatrix} 0 & 1 & 0 & 1 & 1 & 1 & 0 & 0 \\ 1 & 0 & 1 & 0 & 0 & 1 & 1 & 0 \\ 0 & 1 & 0 & 1 & 0 & 0 & 1 & 1 \\ 1 & 0 & 1 & 0 & 1 & 0 & 0 & 1 \\ 1 & 0 & 0 & 1 & 0 & 0 & 0 & 0 \\ 1 & 1 & 0 & 0 & 0 & 0 & 0 & 0 \\ 0 & 1 & 1 & 0 & 0 & 0 & 0 & 0 \\ 0 & 0 & 1 & 1 & 0 & 0 & 0 & 0 \end{bmatrix} = [a_{ij}]$$

$$\text{and } L = \begin{bmatrix} 1 & 0 & 0 & 0 & 0 & 0 & 0 & 0 \\ 0 & 1 & 0 & 0 & 0 & 0 & 0 & 0 \\ 0 & 0 & 1 & 0 & 0 & 0 & 0 & 0 \\ 0 & 0 & 0 & 1 & 0 & 0 & 0 & 0 \\ 0 & 0 & 0 & 0 & 0 & 0 & 0 & 0 \\ 0 & 0 & 0 & 0 & 0 & 0 & 0 & 0 \\ 0 & 0 & 0 & 0 & 0 & 0 & 0 & 0 \\ 0 & 0 & 0 & 0 & 0 & 0 & 0 & 0 \end{bmatrix} = diag(g_i)$$
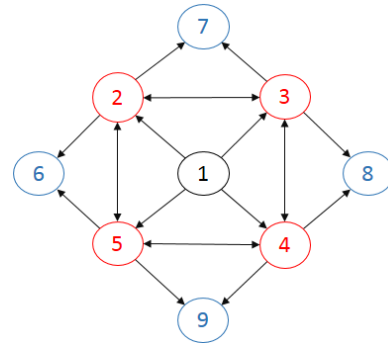
Fig. 2. Communication topology.

The desired distances between the leader and followers were considered as a bias in Eq. (38) as follows.

$$u_i(t) = u_{i1}^c(t) + u_{i2}^c(t) \tag{52}$$

60

$$u_{i1}^c(t) = d_i(t)\left[\sum_{j \in N_i} a_{ij}\left(p_j(t) - p_i(t) + \alpha_{ij}\right)\right.$$

$$\left. - g_i(\varepsilon_i(t) + \beta_i)\right] \tag{53}$$

$$u_{i2}^c(t) = -\sum_{k=1}^{\infty} K_2 \left[\sum_{j \in N_i}\left(a_{ij}\left(p_j(t) - p_i(t)\right.\right.\right.$$

$$\left.\left. + \alpha_{ij}\right) + \gamma_{ij}q_i\right)$$

$$\left. - g_i(\varepsilon_i(t)\beta_i)\right]\delta(t - t_k) \tag{54}$$

where α_{ij} is the distance between ith and jth followers and β_i is the distance between ith follower and the leader.

TABLE I
PARAMETERS OF THE QUADROTORS.

Parameter	m	I_r	I_x	I_y
Value	2.5 kg	6e-5 kg.m^2	0.0433 kg.m^2	0.0433 kg.m^2
Parameter	I_z	h	c_τ	b
Value	0.0465 kg.m^2	0.2 m	0.2 m	3.13e-3 Ns^2/rad^2

A. Scenario One

The simulation was performed for 100 seconds. The quadrotors followed a square path that begins from the center of the square. Five seconds after the simulation started, agent 7 was attacked and 10 seconds after the start, the fault was applied to agent 5 and both remained until the end.

The actual and desired flight path of the leader is shown in Fig. 3. The leader was in the center of the square (O). Then, it took off vertically two meters from the ground (O→A). It moved on half of the diameter of the square (A→B) to reach the first vertex of the square (B). It started flying on a square (B→C→D→E). Then, it came back on half of the other diameter of the square to the center of the square (A). This path was the same for all followers. The actual and desired positions and attitudes of the first quadrotor are shown in Figs. 4 and 5. The obtained results explain that the performance of the leader flight controller in tracking the predefined trajectory is acceptable.
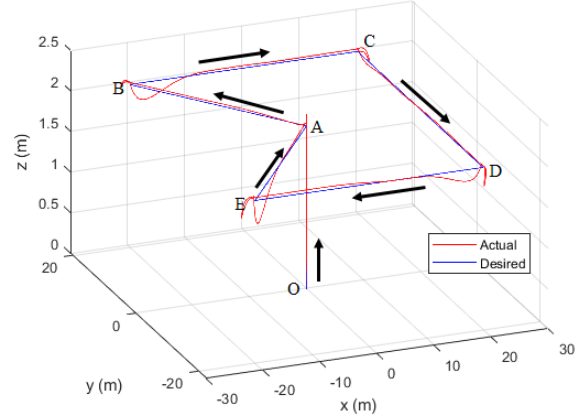
Fig. 3. Scenario One: The actual and desired flight path of the leader quadrotor.
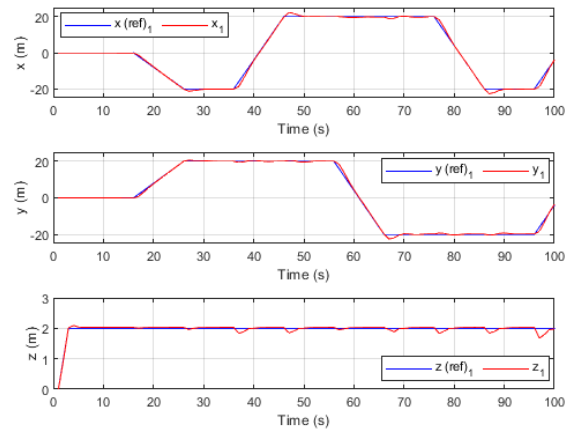
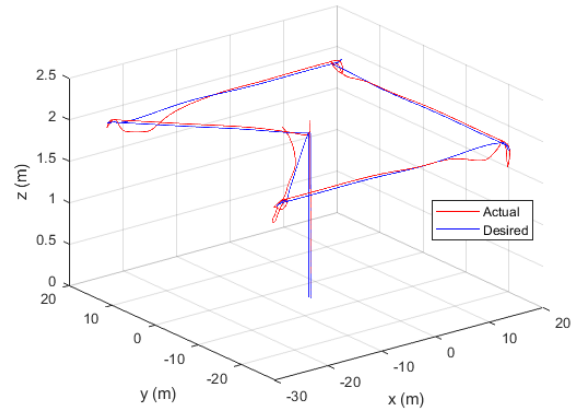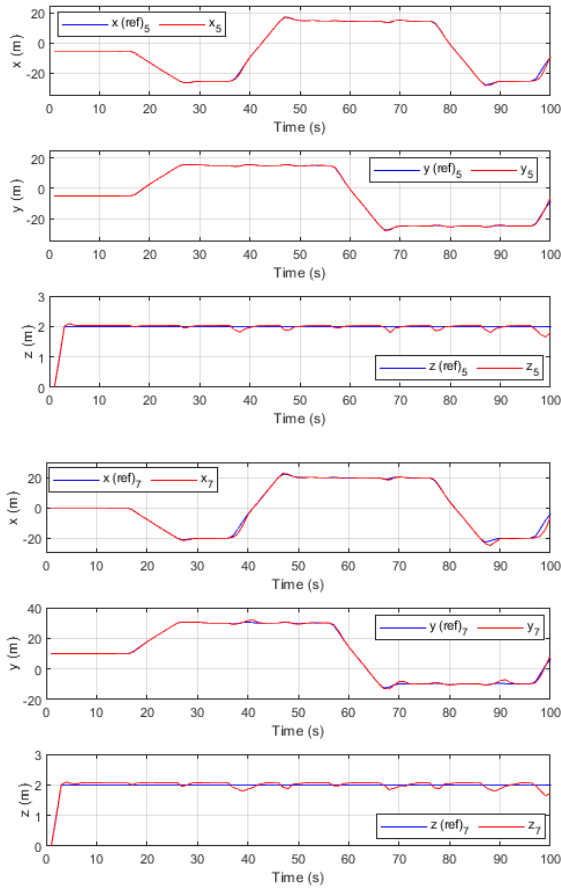Fig. 4. Scenario One: The actual and desired positions of the leader quadrotor.
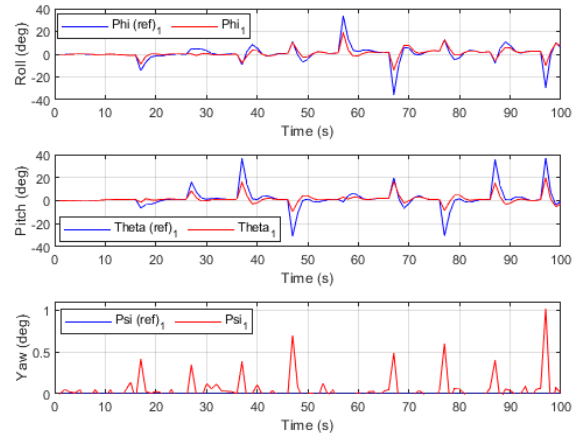
Fig. 5. Scenario One: The actual and desired attitudes of the leader quadrotor.
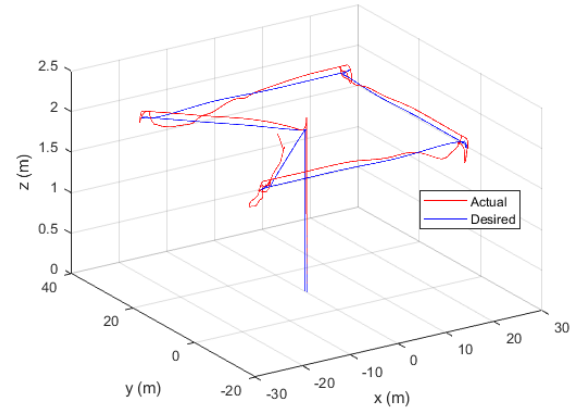
The actual and desired flight path and positions of quadrotors 5 and 7 are given in Fig 6. The obtained results demonstrate that the proposed control method was effective. The quadcopters tracked the reference trajectory in the presence of actuator fault and attack. Fig. 7 shows five snapshots of the simulated formation control. It demonstrates that the formation control was

done, perfectly and the synchronization of quadcopters was achieved. The adapting parameters $d_i(t)$ are given in Fig. 8, which shows that the parameters were adapted

during the flight time from the beginning, and they were bounded.

(a)

(b)

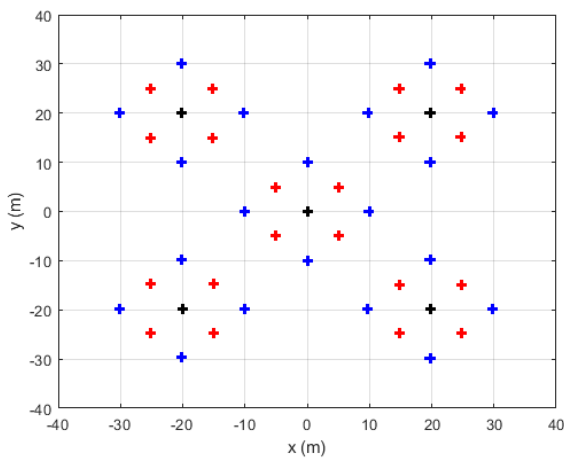Fig. 6. Scenario One: The actual and desired flight path and positions of quadrotor (a) 5 and (b) 7.

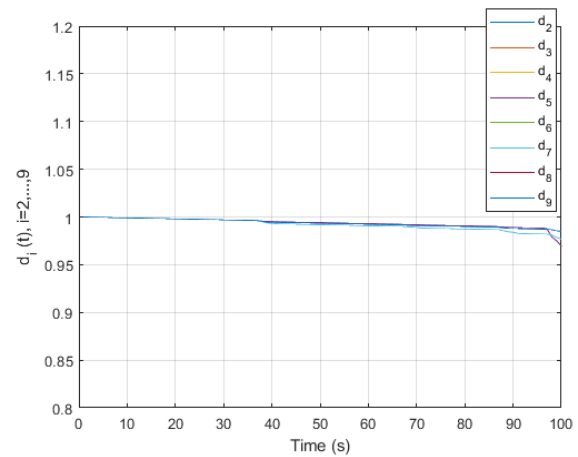Fig. 7. Scenario One: Five snapshots of the simulated quadrotor formation.

Fig. 8. Scenario One: Adapting parameters $d_i(t)$.

For comparison, the results obtained by the proposed control scheme were compared with the conventional method whose control law is defined as

$$u_i\ (t) = -K_2 \left[\sum_{j \epsilon N_i} \left(a_{ij} \left(p_j(t) - p_i(t) \right) \right. \right.$$

$$\left. \left. + \gamma_{ij} q_i \right) - g_i \varepsilon_i(t) \right] + \varphi_i \qquad (55)$$

Fig. 9 shows that the conventional method was not successful in formation control of the followers and the results obtained from it are not acceptable.
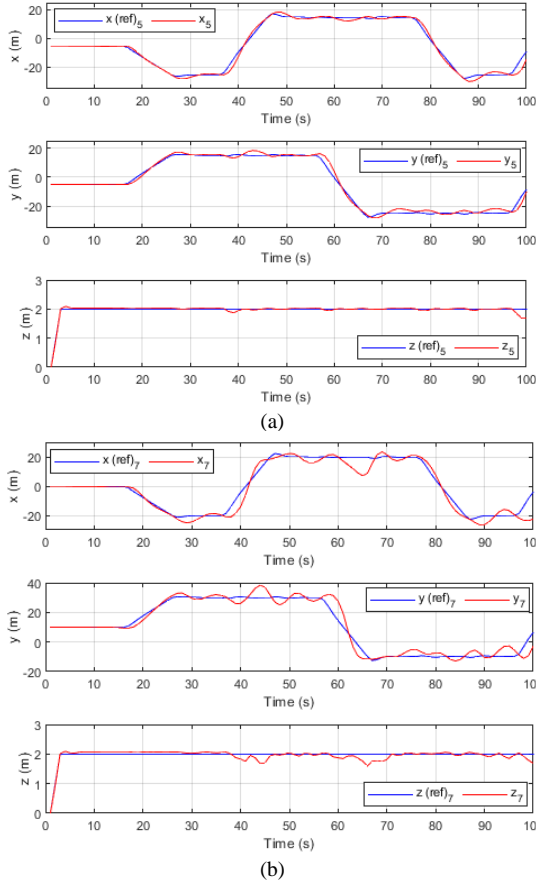
Fig. 9. Scenario One: The actual and desired flight path and positions of quadcopter (a) 5 and (b) 7 obtained by the conventional method.

B. Scenario Two

The simulation was performed for 100 seconds. The quadrotors followed a cylindrical path in a spiral. Five seconds after the simulation started, the fault was applied to agent 6. Ten seconds after the start, agent 4 was attacked and both remained until the end.

The actual and desired flight path of the leader is shown in Fig. 10. The leader took off vertically 2 meters from the ground. It moved on a circle with a diameter of 2 meters and ascended simultaneously to a height of 10 meters. Then, returned vertically to the height of 2

meters. This path is the same for all followers. The actual and desired positions and attitudes of the first quadrotor are given in Figs. 11 and 12. It can be seen that the performance of the leader flight controller in tracking the predefined trajectory is acceptable. The obtained results show that the tracking of the predetermined trajectory for X and Y channels is more challenging than the Z channel.
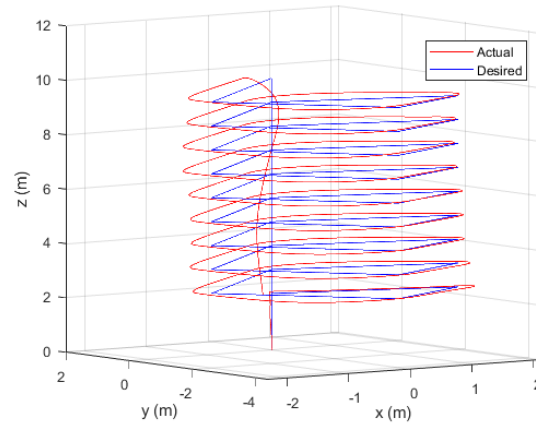

Fig. 10. Scenario Two: The actual and desired flight path of the leader quadrotor.
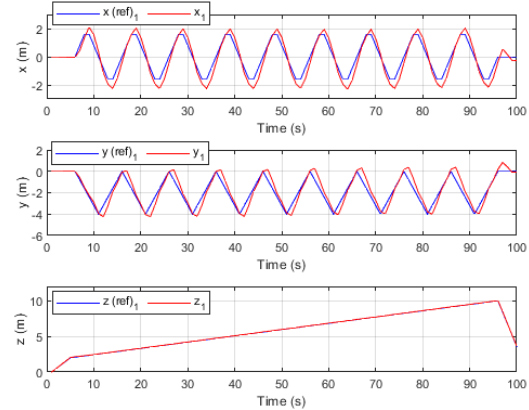

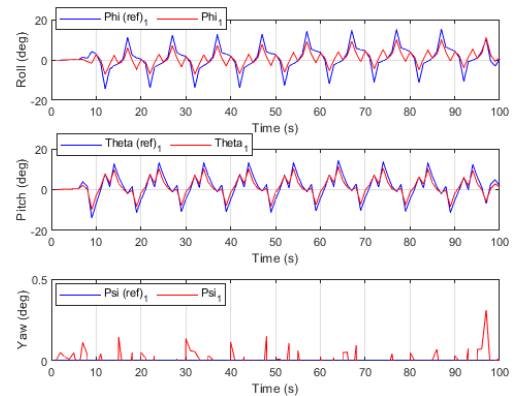Fig. 11. Scenario Two: The actual and desired positions of the leader quadrotor.

Fig. 12. Scenario Two: The actual and desired attitudes of the leader quadrotor.

Fig. 15. Scenario Two: The actual and desired attitudes of the quadcopter (a) 4 and (b) 6.

Fig. 16. Scenario Two: The actual and desired flight path and positions of quadcopter (a) 4 and (b) 6 obtained by the conventional method.
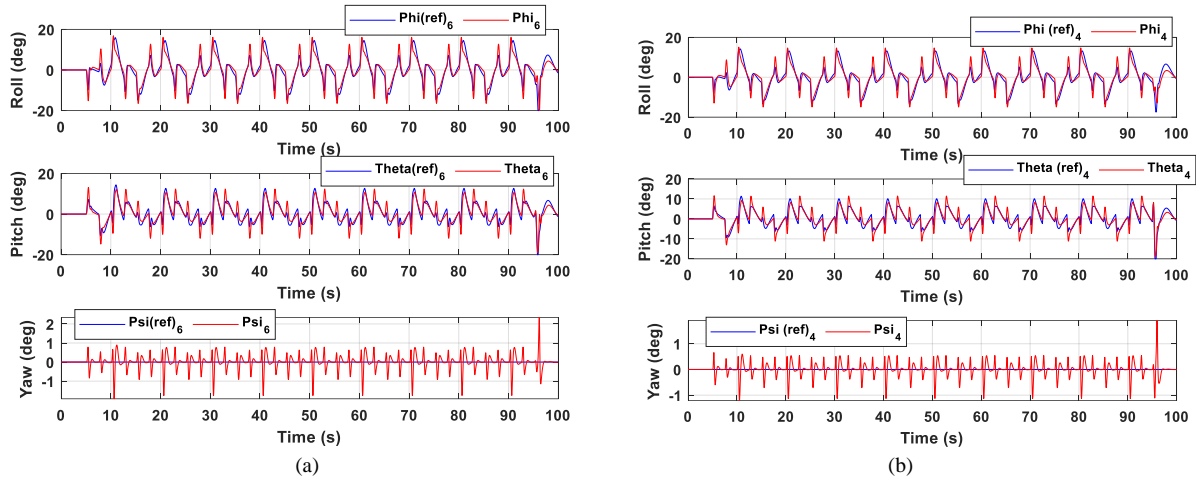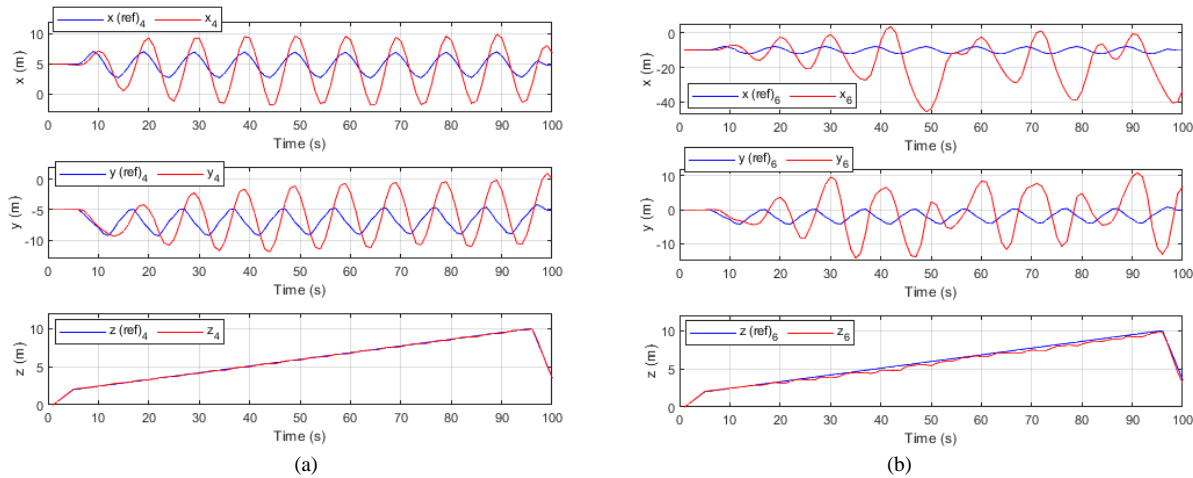
V. CONCLUSION

This paper proposed a cooperative adaptive fault-tolerant formation control for the consensus of MRUAV swarms. The controller was designed to deal with actuator faults and cyber-attacks. The simulation results of two flight scenarios confirmed the effectiveness of the proposed method. It shows that followers could adequately maintain stable flight and achieve swarm formation. Additionally, the impulsive control eliminated the effects of attacks. Notably, although the dynamics of agents were assumed to be a double integrator, the simulation results demonstrated that this is not a limitation of the proposed control scheme. The considered dynamics of the quadcopter in the simulation closely resemble reality. Therefore, we expect similar results in the ongoing experimental studies. The proposed formation control is applicable to any quadcopter swarm whose associated undirected graph is connected, and where at least one follower receives information from the leader quadcopter.

REFERENCES AND FOOTNOTES

[1] A. Mahmood and Y. Kim, "Leader-following formation control of quadcopters with heading synchronization," *Aerospace Science and Technology,* vol. 47, pp. 68-74, 2015.
[2] Q. Ali and S. Montenegro, "Explicit model following distributed control scheme for formation flying of mini UAVs," *IEEE Access,* vol. 4, pp. 397-406, 2016.
[3] Q. Yuan, J. Zhan, and X. Li, "Outdoor flocking of quadcopter drones with decentralized model predictive control," *ISA transactions,* vol. 71, pp. 84-92, 2017.
[4] A. Amrollahi Biyooki, "Distributed Fault Detection in Formation of Multi-Agent Systems with Attack Impact Analysis," Concordia University, 2019.
[5] Z. Wang, J. Yu, S. Lin, J. Dong, and Z. Yu, "Distributed robust adaptive fault-tolerant mechanism for quadrotor UAV real-time wireless network systems with random delay

and packet loss," *IEEE Access,* vol. 7, pp. 134055-134062, 2019.

[6] L. Zhao and G.-H. Yang, "Cooperative adaptive fault-tolerant control for multi-agent systems with deception attacks," *Journal of the Franklin Institute,* vol. 357, no. 6, pp. 3419-3433, 2020.

[7] F. Bordoni and A. D'Amico, "Noise in sensors," *Sensors and Actuators A: Physical,* vol. 21, no. 1-3, pp. 17-24, 1990.

[8] K. Hashimoto, M. Chong, and D. V. Dimarogonas, "Realtime l 1-fault-and-state estimation for multi-agent systems," in *2019 American Control Conference (ACC)*, 2019: IEEE, pp. 1175-1180.

[9] H. Liu, Y. Li, and Z. Wang, "Optimal Guaranteed Cost Control for Multi-agent Systems with Actuator Faults," in *2018 IEEE International Conference on Systems, Man, and Cybernetics (SMC)*, 2018: IEEE, pp. 2001-2006.

[10] T. Wu, J. Hu, and D. Chen, "Non-fragile consensus control for nonlinear multi-agent systems with uniform quantizations and deception attacks via output feedback approach," *Nonlinear Dynamics,* vol. 96, no. 1, pp. 243-255, 2019.

[11] L. Zhao and G.-H. Yang, "Fuzzy adaptive fault-tolerant control of multi-agent systems with interactions between physical coupling graph and communication graph," *Fuzzy Sets and Systems,* vol. 385, pp. 20-38, 2020.

[12] M. J. Er, C. Deng, and N. Wang, "A novel fuzzy logic control method for multi-agent systems with actuator faults," in *2018 IEEE International Conference on Fuzzy Systems (FUZZ-IEEE)*, 2018: IEEE, pp. 1-7.

[13] Z. Yu, Y. Zhang, Z. Liu, Y. Qu, and C. Y. Su, "Distributed adaptive fractional-order fault-tolerant cooperative control of networked unmanned aerial vehicles via fuzzy neural networks," *IET Control Theory & Applications,* vol. 13, no. 17, pp. 2917-2929, 2019.

[14] Z. Yu, Y. Zhang, and Y. Qu, "Prescribed performance-based distributed fault-tolerant cooperative control for multi-UAVs," *Transactions of the Institute of Measurement and Control,* vol. 41, no. 4, pp. 975-989, 2019.

[15] Y. Quan, W. Chen, Z. Wu, and L. Peng, "Distributed fault detection and isolation for leader–follower multi-agent systems with disturbances using observer techniques," *Nonlinear Dynamics,* vol. 93, no. 2, pp. 863-871, 2018.

[16] S. Hajshirmohamadi, F. Sheikholeslam, and N. Meskin, "Actuator fault estimation for multi-agent systems: a sliding-mode observer-based approach," in *2019 IEEE Conference on Control Technology and Applications (CCTA)*, 2019: IEEE, pp. 1000-1005.

[17] Z. Yu, Z. Liu, Y. Zhang, Y. Qu, and C.-Y. Su, "Distributed finite-time fault-tolerant containment control for multiple unmanned aerial vehicles," *IEEE Transactions on Neural Networks and Learning Systems,* vol. 31, no. 6, pp. 2077-2091, 2019.

[18] Z. Yu, Y. Qu, and Y. Zhang, "Fault-tolerant containment control of multiple unmanned aerial vehicles based on distributed sliding-mode observer," *Journal of Intelligent & Robotic Systems,* vol. 93, no. 1, pp. 163-177, 2019.

[19] X. Jin and W. M. Haddad, "Adaptive control for multiagent systems with sensor–actuator attacks and stochastic disturbances," *Journal of Guidance, Control, and Dynamics,* vol. 43, no. 1, pp. 15-29, 2020.

[20] X.-Z. Jin, Z. Zhao, and Y.-G. He, "Insensitive leader-following consensus for a class of uncertain multi-agent systems against actuator faults," *Neurocomputing,* vol. 272, pp. 189-196, 2018.

[21] L. Zhao and G.-H. Yang, "End to end communication rate-based adaptive fault tolerant control of multi-agent systems under unreliable interconnections," *Information Sciences,* vol. 460, pp. 331-345, 2018.

[22] C. Chen *et al.*, "Resilient adaptive and H∞ controls of multi-agent systems under sensor and actuator faults," *Automatica,* vol. 102, pp. 19-26, 2019.

[23] Y. Tan, S. Fei, J. Liu, and D. Zhang, "Asynchronous adaptive event-triggered tracking control for multi-agent systems with stochastic actuator faults," *Applied Mathematics and Computation,* vol. 355, pp. 482-496, 2019.

[24] X. Xingguang, W. Zhenyan, R. Zhang, and L. Shusheng, "Time-varying fault-tolerant formation tracking based cooperative control and guidance for multiple cruise missile systems under actuator failures and directed topologies," *Journal of Systems Engineering and Electronics,* vol. 30, no. 3, pp. 587-600, 2019.

[25] C. Chen, K. Xie, F. L. Lewis, S. Xie, and R. Fierro, "Adaptive synchronization of multi-agent systems with resilience to communication link faults," *Automatica,* vol. 111, p. 108636, 2020.

[26] X. Huang and J. Dong, "Reliable cooperative control and plug-and-play operation for networked heterogeneous systems under cyber–physical attacks," *ISA transactions,* vol. 104, pp. 62-72, 2020.

[27] A. Mustafa and H. Modares, "Attack analysis and resilient control design for discrete-time distributed multi-agent systems," *IEEE Robotics and Automation Letters,* vol. 5, no. 2, pp. 369-376, 2019.

[28] Z. Zheng, M. Qian, P. Li, and H. Yi, "Distributed adaptive control for UAV formation with input saturation and actuator fault," *IEEE Access,* vol. 7, pp. 144638-144647, 2019.

[29] X. Wu, Y. Jin, and R. Zhen, "Fault-tolerant Time-varying Formation Tracking Control for Unmanned Aerial Vehicle Swarm Systems with Switching Topologies and a Leader of Unknown Control Input," in *2021 4th International Conference on Intelligent Autonomous Systems (ICoIAS)*, 2021: IEEE, pp. 265-270.

[30] G. Wen, X. Zhai, Z. Peng, and A. Rahmani, "Fault-tolerant secure consensus tracking of delayed nonlinear multi-agent systems with deception attacks and uncertain parameters via impulsive control," *Communications in nonlinear science and numerical simulation,* vol. 82, p. 105043, 2020.

[31] X. Dong, Y. Li, C. Lu, G. Hu, Q. Li, and Z. Ren, "Time-varying formation tracking for UAV swarm systems with switching directed topologies," *IEEE transactions on neural networks and learning systems,* vol. 30, no. 12, pp. 3674-3685, 2018.

[32] R. Deng, J. Chen, M. Wang, Z. Shi, and Y. Zhong, "Fault Detection and Isolation for a Fixed-wing UAV Swarm System with Uncertainties and Disturbances," in *2019 Chinese Control Conference (CCC)*, 2019: IEEE, pp. 4919-4924.

[33] H. Yang, B. Jiang, V. Cocquempot, and M. Chen, "Spacecraft formation stabilization and fault tolerance: A state-varying switched system approach," *Systems & control letters,* vol. 62, no. 9, pp. 715-722, 2013.

[34] B. Wang, J. Wang, B. Zhang, W. Chen, and Z. Zhang, "Leader–follower consensus of multivehicle wirelessly networked uncertain systems subject to nonlinear dynamics and actuator fault," *IEEE Transactions on Automation Science and Engineering,* vol. 15, no. 2, pp. 492-505, 2017.

[35] K. Yuhang *et al.*, "Robust leaderless time-varying formation control for unmanned aerial vehicle swarm system with Lipschitz nonlinear dynamics and directed switching topologies," *Chinese Journal of Aeronautics,* vol. 35, no. 1, pp. 124-136, 2022.

[36] J. Hu, H. Niu, J. Carrasco, B. Lennox, and F. Arvin, "Fault-tolerant cooperative navigation of networked UAV swarms for forest fire monitoring," *Aerospace Science and Technology,* vol. 123, p. 107494, 2022.

66

[37] J. Ajmera and V. Sankaranarayanan, "Point-to-point control of a quadrotor: Theory and experiment," *IFAC-PapersOnLine,* vol. 49, no. 1, pp. 401-406, 2016.

[38] R. W. Beard, "Quadrotor dynamics and control," *Brigham Young University,* vol. 19, no. 3, pp. 46-56, 2008.

[39] D. Lara, A. Sanchez, R. Lozano, and P. Castillo, "Real-time embedded control system for VTOL aircrafts: Application to stabilize a quad-rotor helicopter," in *2006 IEEE Conference on Computer Aided Control System Design, 2006 IEEE International Conference on Control Applications, 2006 IEEE International Symposium on Intelligent Control*, 2006: IEEE, pp. 2553-2558.

[40] Y. Wu and J. Dong, "Controller synthesis for one-sided Lipschitz Markovian jump systems with partially unknown transition probabilities," *IET Control Theory & Applications,* vol. 11, no. 14, pp. 2242-2251, 2017.

[41] X. Mao, "Stability of stochastic differential equations with Markovian switching," *Stochastic processes and their applications,* vol. 79, no. 1, pp. 45-67, 1999.